JOC Note
pubs.acs.org/joc

Thermal Degradation of Methyl β-D-Glucoside. A Theoretical Study of Plausible Reaction Mechanisms

Takashi Hosoya,[†] Yoshihide Nakao,[†] Hirofumi Sato,[†] Haruo Kawamoto,[‡] and Shigeyoshi Sakaki*,[†]

[†]*Department of Molecular Engineering, Graduate School of Engineering, Kyoto University, Kyotodaigaku-katsura, Nishikyo-ku, Kyoto 615-8510, Japan, and* [‡]*Department of Socio-Environmental Energy Science, Graduate School of Energy Science, Kyoto University, Yoshida-honmachi, Sakyo-ku, Kyoto 606-8501, Japan*

sakaki@moleng.kyoto-u.ac.jp

Received February 27, 2009

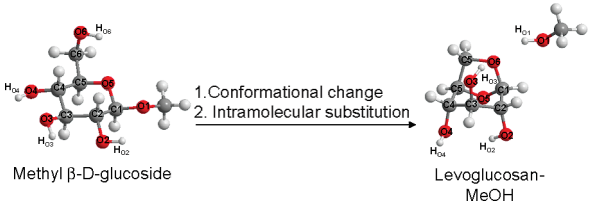

Thermal conversion of methyl β-D-glucoside to levoglucosan was studied with the MP4//DFT(B3LYP) method. The first step is conformational change of the reactant to $^1C_4$ from $^4C_1$. The second step is intramolecular nucleophilic substitution at the anomeric C1, which occurs via one step without oxacarbenium ion intermediate. The $\Delta G^{0\ddagger}$ value (52.5 kcal/mol) is smaller than the C1−O1 bond energy, indicating the direct homolysis mechanism is clearly ruled out. Bimolecular reaction also occurs with smaller activation energy via the similar transition state.

Thermal degradation of β-D-glucoside without any solvent and catalyst induces a transglycosylation reaction to produce a considerable amount of levoglucosan (1,6-anhydro-β-D-glucopyranose).[1−6] This reaction is a fundamental process in various thermal conversions of woody biomass resources[2,3] and thermal saccharification of cellulose, also.[3] The product, levoglucosan, is important also in environmental science as a molecular marker for aerosols and charcoals.[7] However, the mechanism of this reaction has not been elucidated yet. Several groups proposed an ionic mechanism, in which the reaction occurs via oxacarbenium ion intermediate (Scheme 1).[4] This intermediate is further converted to levoglucosan through nucleophilic attack of O6 to C1. Protonation of O1 and the important role of oxacarbenium ion were also experimentally and theoretically proposed.[8] Other groups proposed a direct homolysis mechanism, in which homolytic cleavage of the glycosidic bond is the initial step (Scheme 1).[5] The argument of these two mechanisms has continued due to the lack of clear evidence. In this study we theoretically investigated the reaction mechanism of levoglucosan production from methyl β-D-glucoside with the MP4//DFT(B3LYP) method; see Scheme 2 for the reaction examined. Our purpose is to present a clear conclusion about the reaction mechanism and a deep understanding of the reaction.

The GAUSSIAN 03 program package[9] was employed here. The DFT with the B3LYP functional[10] was used for the geometry optimization. The 6-31 + G(d) basis sets were used for C and O, and the 6-31G(p) basis set was used for H. This basis set system is named BS-I, hereafter. We ascertained that each equilibrium geometry exhibited no imaginary frequency and each transition state exhibited one imaginary frequency. We carried out IRC calculation, to check that the transition state connected reactant and product. Potential energy changes were evaluated by the MP4(SDTQ) method with the DFT-optimized geometries, where a better basis set system (BS-II) was used. In BS-II, the 6-311G(d) basis sets were used for all atoms, where a diffuse function was added to O and a p-polarization function was added to H of OH groups. The Gibbs energy change (ΔG^0) was evaluated at 600 K and 1 atm with the MP4(SDTQ)/BS-II-evaluated potential energy and the

(1) (a) Shafizadeh, F. *J. Anal. Appl. Pyrolysis* **1982**, *3*, 283. (b) Antal, M. J., Jr. *Adv. Solar Energy* **1983**, *1*, 61. (c) Shafizadeh, F. *Adv. Carbohydr. Chem.* **1968**, *23*, 219. (d) Emsley, A. M.; Stevens, G. C. *Cellulose* **1994**, *1*, 26. (e) Mamleev, V.; Bourbigot, S.; Bras, M. L.; Yvon, J. *J. Anal. Appl. Pyrolysis* **2009**, *84*, 1. (f) Evans, R. J.; Milne, T. A. *Energy Fuels* **1987**, *1*, 123. (g) Furneaux, R. H.; Shafizadeh, F. *Carbohydr. Res.* **1979**, *74*, 354. (h) Richards, G. N.; Shafizadeh, F. *Carbohydr. Res.* **1982**, *106*, 83.

(2) Huber, G. W.; Iborra, S.; Corma, A. *Chem. Rev.* **2006**, *106*, 4044.

(3) (a) Shafizadeh, F.; Furneaux, R. H.; Cochran, T. G.; Scholl, J. P.; Sakai, Y. *J. Appl. Polym. Sci.* **1979**, *23*, 3525. (b) Kwon, G.-J.; Kuga, S.; Hori, K.; Yatagai, M.; Ando, K.; Hattori, N. *J. Wood Sci.* **2006**, *52*, 461. (c) Kwon, G.-J.; Kim, D.-Y.; Kimura, S.; Kuga, S. *J. Anal. Appl. Pyrolysis* **2007**, *80*, 1. (d) Radlein, D.; Piskorz, J; Scott, D. S. *J. Anal. Appl. Pyrolysis* **1991**, *19*, 41. (e) Piskorz, J.; Majerski, P.; Radlein, D.; Vladars-Usas, A.; Scott, D. S. *J. Anal. Appl. Pyrolysis* **2000**, *56*, 145. (f) Piskorz, J.; Radlein, D.; Scott, D. S. *J. Anal. Appl. Pyrolysis* **1989**, *16*, 127.

(4) (a) Essig, M. G.; Richards, G. N.; Schenck, E. M. In *Cellulose and Wood, Proceedings of the 10th Cellulose Conference: Syracuse, NY*; Schuerch, C., Ed.; Wiley; New York, 1988, pp 841−862. (b) Ponder, G. R.; Richards, G. N *Biomass Bioenergy* **1994**, *7*, l. (c) Ponder, G. R.; Richards, G. N.; Stevenson, T. T. *J. Anal. Appl. Pyrolysis* **1992**, *22*, 217. (d) Lowary, T. L.; Richards, G. N. *Carbohyd. Res.* **1990**, *198*, 79. (e) Shafizadeh, F.; Susott, R. A.; McGinnis, G. D. *Carbohyd. Res.* **1972**, *22*, 63. (f) Köll, P.; Borchers, G.; Metzger, J. O. *J. Anal. Appl. Pyrolysis* **1991**, *19*, 119.

(5) (a) Madorsky, S. L.; Hart, V. E.; Straus, S. *J. Res. Nat. Bur. Stand.* **1956**, *56*, 343. (b) Pakhomov, A. M. *Izv. Akad. Nauk SSSR, Ser. Khim.* **1957**, 1497. (c) Kislitsyn, A. N.; Rodionova, Z. M.; Guseva, A. V.; Gusarskaya, N. L. *Sb. Tsentr. Nauchno-Issled. Proekt. Inst. Lesokhim. Prom.* **1971**, *21*, 4.

(6) (a) Arseneau, D. F. *Can. J. Chem.* **1971**, *49*, 632. (b) Shafizadeh, F.; Fu, Y. L. *Carbohydr. Res.* **1973**, *29*, 113. (c) Yang, H.; Yan, R.; Chen, H. P.; Lee, D. H.; Zheng, C. G. *Fuel* **2007**, *86*, 1781. (d) MOK, W. S.-L.; Antal, M. J., Jr. *Thermochim. Acta* **1983**, *68*, 165.

(7) (a) Schkolnik, G.; Rudich, Y. *Anal. Bioanal. Chem.* **2006**, *385*, 26. (b) Simoneit, B. R. T. *Appl. Geochem.* **2002**, *17*, 129. (c) Kuo, L.-J.; Herbert, B. E.; Louchouarn, P. *Org. Geochem.* **2008**, *39*, 1466.

(8) (a) Whitfield, D. M.; Nukada, T. *Carbohydr. Res.* **2007**, *342*, 1291. (b) Andrei, R.; Ionescu, D. M.; Whitfield, M. Z.; Nukada, T *Carbohydr. Res.* **2006**, *341*, 2912. (c) Bennet, A. J.; Sinnott, M. L. *J. Am. Chem. Soc.* **1986**, *108*, 7287. (d) Timell, T. E. *Can. J. Chem.* **1964**, *42*, 1456.

(9) Pople, J. A. et al. *Gaussian 03*, Revision C.02; Gaussian, Inc.: Wallingford, CT, 2004. See the SI for the complete reference.

(10) (a) Becke, A. D. *Phys. Rev. A* **1988**, *38*, 3098. (b) Becke, A. D. *J. Chem. Phys.* **1983**, *98*, 5648.

DOI: 10.1021/jo900457k Published on Web 07/27/2009

SCHEME 1. Direct Homolysis and Ionic Mechanisms

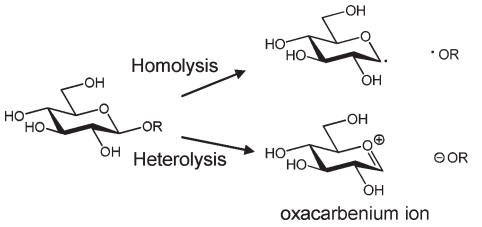

SCHEME 2. Reaction Investigated in This Study

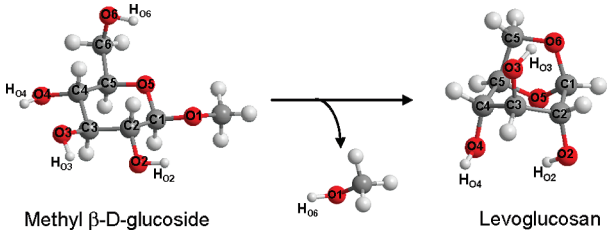

DFT/BS-I-evaluated zero-point energy, thermal energy, and entropy change. Pictures of molecular orbitals were drawn with the MOLEKEL program.[11]

In the direct homolysis mechanism, the first step is the homolytic cleavage of the glycosidic C1−O1 bond. We evaluated bond dissociation energies (BDEs) of the glycosidic bonds in the reactant (methyl β-D-glucoside) and the product (levoglucosan). The MP4(SDTQ)-calculated C1−O1 BDE is 91.8 (65.4) and 91.3 (84.6) kcal/mol in the reactant and the product, respectively, where the Gibbs energy changes for the C1−O1 bond cleavage are given in parentheses (Scheme S1, SI).

In the ionic mechanism, the glycosidic C1−O1 bond cleavage occurs in a heterolytic manner. The heterolytic C1−O1 bond energy is very large (189.5 kcal/mol; see Scheme S2 in the SI), indicating that the heterolytic bond cleavage is difficult. Thus, the ionic mechanism via concerted C1−O1 bond cleavage was investigated here, in which four kinds of pathway A−D were found (Figures 1 and 2). Pathway A (the red lines) is the most favorable, while pathways B−D need a larger activation barrier than does pathway A. We also investigated the other reaction courses in which the O2H and O3H groups play the role of proton donor. However, these reaction courses are ruled out because of their large activation barriers (Figure S1, SI). The Gibbs activation energy ($\Delta G^{0\ddagger}$) of pathway A was calculated to be 52.5 kcal/mol at 600 K and 1 atm (Figure 1), which is much smaller than the ΔG^0 value for the C1−O1 bond cleavage (see above). Thus, it should be clearly concluded that the concerted ionic mechanism is more favorable than the direct homolysis of the glycosidic bond.

Hereafter, we wish to focus on the concerted ionic mechanism. The first step is the conformational changes of the pyranosyl ring of methyl β-D-glucoside to afford $^1C_4$ from $^4C_1$ via $B_{3,O}$ (Figures 1 and 2), where $^4C_1$ is the predominant ring conformation. Though $B_{3,O}$ is not an equilibrium structure in simple tetrahydropyran, it becomes an equilibrium structure in methyl β-D-glucoside because of the hydrogen bond network among the OH groups like β-D-glucose[12a] and α-L-idose.[12d] This conformational change occurs through the two transition states, $\mathbf{TS_{C1}}$ and $\mathbf{TS_{C2}}$, $\Delta G^{0\ddagger}$ values of which are 7.8 and 17.3 kcal/mol, respectively (Figure 1). Hydroxymethyl rotamers at the sixth position are maintained as the *gg*-type during this conformational transition. Though the experimental $\Delta G^{0\ddagger}$ value has not been reported, the present value is similar to the previous values calculated for the conformational changes of several sugar molecules.[12]

After the conformational changes, the resulting *gg*-$^1C_4$ conformer undergoes nucleophilic substitution at the anomeric C1 to form the product complex **P1**, which consists of the levoglucosan and methanol molecules. **P1** then releases methanol and levoglucosan molecules. This step increases entropy, with which overall reaction becomes exothermic. The exothermicity was calculated to be −1.1 kcal/mol based on Gibbs energy change at 600 K and 1 atm (Figure 1). In the other pathways B−D starting from *gt*-$^1C_4$, *gg*-$B_{3,O}$, and *gt*-$B_{3,O}$ conformers (Figures 1 and 2), the $\Delta G^{0\ddagger}$ values (59.3−67.1 kcal/mol) are considerably larger than that of pathway A. These higher activation energies are interpreted in terms of the H6···O1 hydrogen bond; these *gt*-$^1C_4$, *gg*-$B_{3,O}$, and *gt*-$B_{3,O}$ have a longer O6H···O1 hydrogen bond than does the *gg*-$^1C_4$, which requires larger activation energy for the proton transfer (Figure S2, SI). No pathway starting from *tg*-rotamers (the other type of hydroxymethyl rotamer) was found, because the *tg*-$B_{3,O}$ and *tg*-$^1C_4$ do not have the O6H···O1 hydrogen bond (Figure S2, SI).

The nucleophilic substitution at the anomeric C1 is the most important process in the whole reaction pathway. To obtain detailed knowledge about this process, IRC calculation was carried out in pathway A; see Scheme S3 in the SI for detailed geometry changes. As shown in Figure 3A, C1−O1 is considerably elongated upon going to transition state $\mathbf{TS_{S1}}$ from the reactant (*gg*-$^1C_4$) and then moderately elongated upon going to **P1** from $\mathbf{TS_{S1}}$. On the other hand, the C1−O6 distance moderately shortens upon going to $\mathbf{TS_{S1}}$ from the reactant (*gg*-$^1C_4$) and then considerably shortens upon going to **P1** from $\mathbf{TS_{S1}}$. Interestingly, the O6−H_{O6} bond is considerably elongated concomitantly with the O1−H_{O6} bond shortening before $\mathbf{TS_{S1}}$. These results indicate that this reaction occurs in one step but three important events are involved. The first event is the C1−O1 bond cleavage that is almost completed around $\mathbf{TS_{S1}}$ to form methanol. The second event is the proton transfer from O6 to O1, which occurs before $\mathbf{TS_{S1}}$ when the C1−O1 bond is elongated to about 2.0 Å. The importance of the similar protonation at O1 was also proposed in other bimolecular glycosylation,[8] though unimolecular protonation occurs here. The final event is the C1−O6 bond formation that occurs after $\mathbf{TS_{S1}}$.

As shown in Figure 3B, the negative charge of O1 starts to increase along with the C1−O1 elongation at the initial stage of the nucleophilic substitution, which induces the

(11) Flükiger, P.; Lüthi, H. P.; Portann, S.; Weber, J. *MOLEKEL*, v.4.3; Scientific Computing: Manno, Switzerland, 2002−2002. Portman, S.; Lüthi, H. P. *CHIMIA* **2000**, *54*, 766.

(12) (a) Biarnés, X.; Ardévol, A.; Planas, A.; Rovira, C.; Laio, A.; Parrinello, M. *J. Am. Chem. Soc.* **2007**, *129*, 10686. (b) Ionescu, A. R.; Bérces, A.; Zgierski, M. Z.; Whitfield, D. M.; Nukada, T. *J. Phys. Chem. A* **2005**, *109*, 8096. (c) O'Donoghue, P.; Luthey-Schulten, Z. A. *J. Phys. Chem. B* **2000**, *104*, 10398. (d) Kurihara, Y.; Ueda, K. *Carbohydr. Res.* **2006**, *341*, 2565.

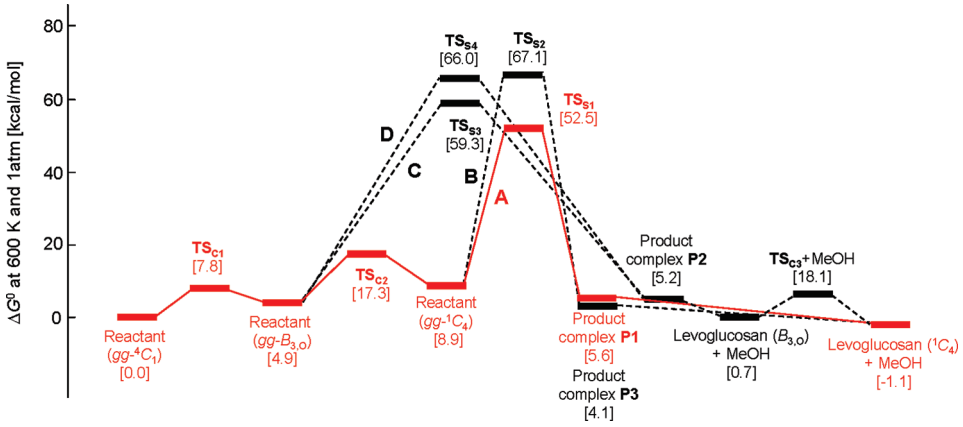

FIGURE 1. Gibbs energy changes in the ionic reaction from methyl β-D-glucoside to levoglucosan calculated with the MP4(SDTQ)/BS-II//DFT(B3LYP)/BS-I method.

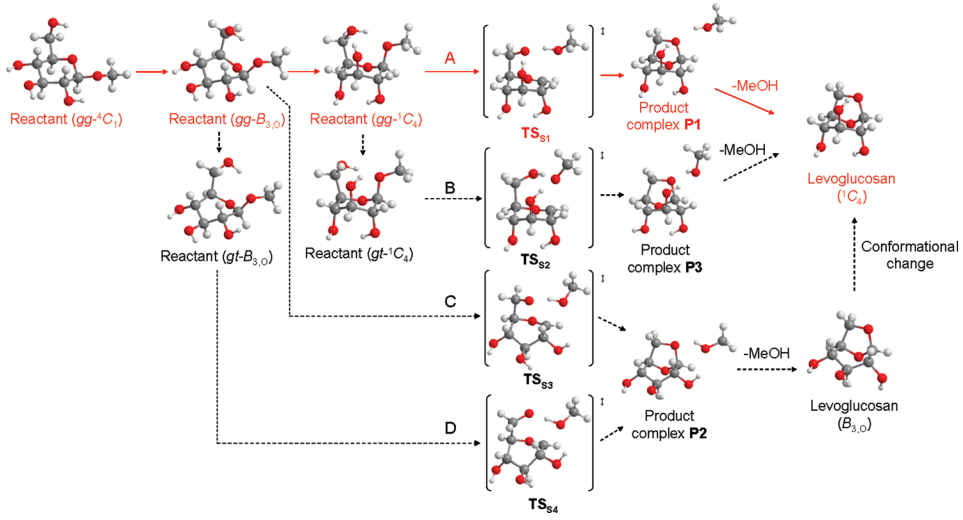

FIGURE 2. Geometry changes in the reaction from methyl β-D-glucoside to levoglucosan calculated with the DFT(B3LYP)/BS-I method.

subsequent proton transfer from O6 to O1. This proton transfer considerably increases the negative charge of O6 and the positive charge of C1. As a result, the reaction system involves the anionic O6 and the cationic C1 atoms. This electronic structure is essentially the same as that of the oxacarbenium ion intermediate (Scheme 1). It is noted that the negative charge of O5 considerably decreases upon going to $\mathbf{TS_{S1}}$ from the reactant (gg-$^1C_4$). This is understood in terms of intramolecular charge transfer (CT) from O5 to C1, which stabilizes the cationic C1 center. Though the negative charge of O1 considerably decreases upon going from the reactant to $\mathbf{TS_{S1}}$, it stops to change around $\mathbf{TS_{S1}}$. This is because the O1−H_{O6} bond formation occurs before $\mathbf{TS_{S1}}$ and the C1−O1 bond breaking occurs around $\mathbf{TS_{S1}}$. After $\mathbf{TS_{S1}}$, the nucleophilic attack of O6 to C1 occurs, as described above, which decreases the negative charge of O6 and the positive charge of C1 upon going to **P1** from $\mathbf{TS_{S1}}$. Simultaneously, the negative charge of O5 considerably increases, indicating the polarization among C1, O5, and O6 becomes smaller by the C1−O6 bond formation.

The HOMO and the HOMO-1 of $\mathbf{TS_{S1}}$ mainly consist of two lone pairs of O6 (Figure 4), one of which is formed by the proton transfer from O6 to O1, as shown in Scheme 3. These results are consistent with the considerably large negative charge of O6 around $\mathbf{TS_{S1}}$. The HOMO-22 mainly consists of the O5 lone pair, which interacts with the empty p orbital of C1 in a bonding way (Scheme 3), indicating the presence of π-type interaction, which corresponds to the intramolecular CT from O5 to C1. The similar CT has been proposed in the oxacarbenium ion intermediate (Scheme 1).[4,8] The LUMO largely consists of the C1 p orbital into which the O5 p orbital mixes in an antibonding way. As a result, the π*-type interaction is clearly observed in the LUMO. The nucleophilic attack of O6 to C1 is understood to occur through the intramolecular CT from the HOMO mainly consisting of the O6 lone pair to the LUMO mainly consisting of the C1 p orbital.

We also investigated the bimolecular ionic mechanism in which the second β-D-glucoside plays the role of proton donor (Figure 5). The DFT(B3LYP)/BS-II-calculated $\Delta G^{0\ddagger}$ value is 36.4 kcal/mol for this reaction and 47.7 kcal/mol for pathway A (Table S2, SI). In the transition state, H'_{O6} has already moved to the O1 atom to form methanol, and the H_{O6} has already moved to the O6′ atom to form the OH bond, while the C1−O6 distance is still long. This feature is essentially the same as $\mathbf{TS_{S1}}$ of pathway A. In other words, the oxacarbenium ion is not found in the bimolecular

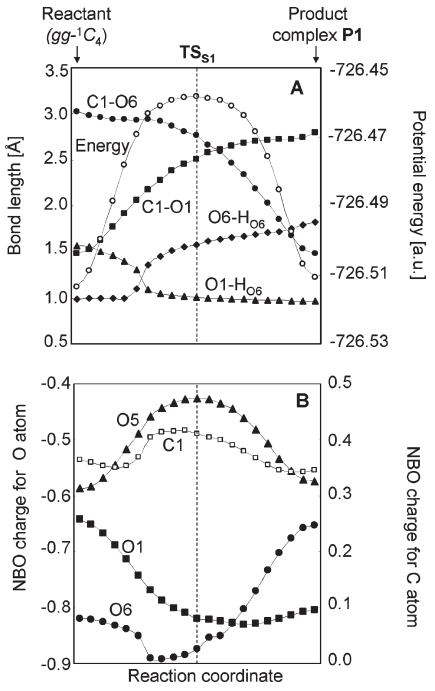

FIGURE 3. Changes of bond distances (A) and NBO charges (B) from the methyl β-D-glucoside (gg-$^1C_4$) to the product complex **P1** via $\mathbf{TS_{S1}}$ calculated with the DFT(B3LYP)//BS-I method.

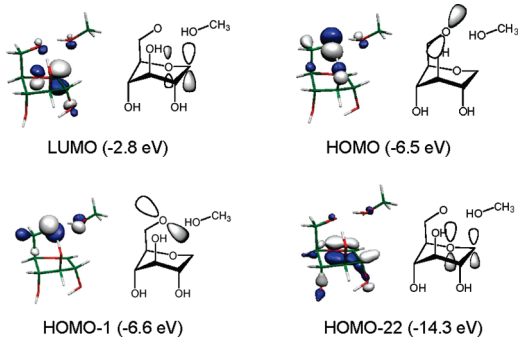

FIGURE 4. Several important Kohn−Sham orbitals of $\mathbf{TS_{S1}}$ and the orbital energies calculated with the DFT(B3LYP)/BS-I method.

SCHEME 3. Changes in Molecular Orbitals during the Substitution

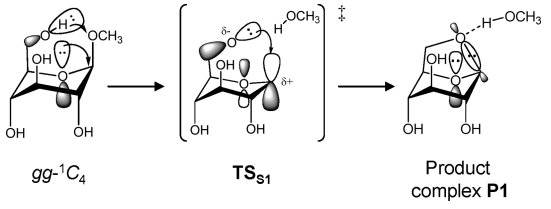

reaction but the electronic structure of the transition state is essentially the same as that of the oxacarbenium ion; see Figure S4 in the SI for details. Other bimolecular pathways, in which the O2′H, O3′H and O4′H play a role of proton donor (Figure S5, SI), need larger activation energy. These bimolecular reactions are similar to the acid-catalyzed cleavage of the glycosidic bond.[8]

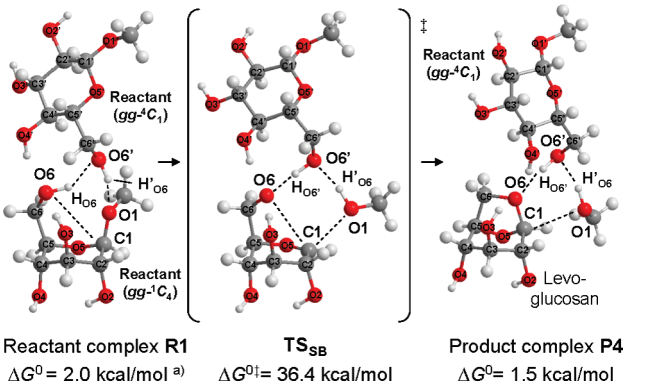

FIGURE 5. Changes in geometry and Gibbs energy in the bimolecular pathway, where energy was evaluated with the DFT(B3LYP)/BS-II method. Footnote a: Relative to monomeric gg-$^4C_1$.

In summary, the concerted ionic mechanism is more favorable than the direct homolysis of the glycosidic bond. In this mechanism, the reaction occurs via two steps. The first step is the conformational change of methyl β-D-glucoside from $^4C_1$ conformer to $^1C_4$. The second step is the intramolecular substitution at the anomeric carbon to form the product. Unlike the ionic mechanism previously proposed (Scheme 1), the oxacarbenium ion intermediate is not formed, though the electronic structure of the transition state is essentially the same as that of the oxacarbenium ion intermediate. In the substitution step, three events are involved: the C1−O1 bond cleavage, the proton transfer from O6 to O1, and the nucleophilic attack of O6 to C1. The bimolecular ionic mechanism is more favorable because the OH group of the second methyl β-D-glucoside participates in smooth proton transfer. It is noted that these reaction features of methyl β-D-glucoside would not be exactly the same as those of real cellulose.

Acknowledgment. This work was financially supported by a Grant-in-Aid for JSPS Fellows (No. 20.1219), Grant-in-Aids on basic research (No. 21350009), Priority Areas for "Molecular Theory for Real Systems" (No. 461), and Creative Scientific Research, NAREGI project from the Ministry of Education, Science, Sports, and Culture. SGI Altix4700 workstations of Institute for Molecular Science (Okazaki, Japan) and PC cluster computers of our laboratory were used.

Supporting Information Available: The complete description of ref 9; geometry changes of the minor pathways F−I (Figure S1); optimized geometries of gg-$^1C_4$, gt-$^1C_4$, gg-$B_{3,O}$, and gt-$B_{3,O}$ conformers (Figure S2); changes of geometries and atomic charges in the pathways B−D (Figure S3) and the bimolecular pathway (Figures S4 and S5); homolytic and heterolytic cleavage of the C1−O1 bond (Schemes S1 and S2); geometry changes in pathway A (Scheme S3); homolytic BDE evaluated with DFT and MP2 to MP4(SDTQ) methods (Table S1); $\Delta G^{0‡}$ values of pathways A−D evaluated with DFT and MP2 to MP4(SDTQ) methods (Table S2); and Cartesian coordinates of all species (Tables S3−S19). This material is available free of charge via the Internet at http://pubs.acs.org.